Nonlinear frequency response based identification and adaptive control for a class of nonlinear systems

Yu Tang
tang@unam.mx
National Autonomous University of Mexico

October 10, 2017

Outline

Motivations

For LTI, asymptitical stable systems, Frequency Response Function (FRF) are useful for

- System identification: parametric and nonparametric identification.
- Performance and robustness characterization: frequency resonance, phase and gain margin, Nyquist criterion.
- Controller designs: frequency response compensation, frequency response shaping.

Motivations

For nonlinear systems, FRF are less understood, because

- The solution depends on the initial condition.
- For a given input, there may exist multiple solutions.

Some approximation methods exist, such as

- Describing function:
  - to characterize static nonlinearities (saturation, rely, dead zone, hysteresis).
  - to predict the existence of limit cycle.
- Generalized frequency response function: limited to second order nonlinear systems.

In general,

- No-exact FRF were defined for nonlinear systems.
- Lacking frequency domain methods to analysis nonlinear systems.

Frequency response function (FRF)

FRF for *linear* system

Consider an LTI system

$$\begin{aligned} \dot{x} &= Ax + Bu, \quad x(0) = x_0 \\ y &= Cx \end{aligned} \tag{1}$$

where $x \in \mathbb{R}^n$ is the state vector, $u, y \in \mathbb{R}$ is the system input and output, respectively, A, B, C are constant matrices with appropriate dimensions. The system is asymptotically stable, *i.e.*, there exist symmetric matrices $P > 0$ and $Q > 0$ such that

$$A^T P + PA = -Q \tag{2}$$

FRF for *linear* system

Then under a harmonic excitation $u = a\sin(\omega t) = Im(ae^{i\omega}t)$ there exists a unique steady-state solution $\bar{x}(t) = \lim_{t\to\infty} x(t)$ and is given by

$$\bar{x}(t) = Im(G(i\omega)ae^{i\omega}) = a|G(i\omega)|sin(\omega t + argG(i\omega)) \tag{3}$$

where $G(i\omega) = G(s = i\omega)$ and $G(s) = (sI - A)^{-1}B$ is the system transfer function.

However, this method can not be extended to nonlinear systems, because the transfer function is not defined for nonlinear systems.

FRF for *linear* system

Consider the internal model for the harmonic input:

$$\begin{aligned} \dot{v} &= S(\omega)v \\ u &= \Gamma v \end{aligned}$$

where

$$v = \begin{bmatrix} v_1 \\ v_2 \end{bmatrix}, \; S(\omega) = \begin{bmatrix} 0 & \omega \\ -\omega & 0 \end{bmatrix}, \; \Gamma = [1 \; 0]$$

which in cascade with the LTI system

$$\dot{x} = Ax + Bu$$

produces the steady-state solution $\bar{x} := \alpha(v, \omega) = \Pi(\omega)v$.

FRF for *linear* system

The matrix $\Pi(\omega)$ cab be obtained by solving the Lyapunov equation

$$\Pi(\omega)S(\omega) - A\Pi(\omega) = B\Gamma \tag{4}$$

Since A and $S(w)$ have no common eigenvalues, there exists a unique solution $\Pi(w)$ for any given B and Γ, and turns to be

$$\Pi(w) = [Re(G(i\omega)) \; Im(G(i\omega))]$$

For LTI systems, this FRF depends on only the frequency w, not on the amplitude a.

FRF for *nonlinear* system

Consider an nonlinear time invariant system

$$\begin{aligned} \dot{x} &= f(x,u), \quad x(0) = x_0 \\ y &= h(x) \end{aligned} \tag{5}$$

where $x \in \mathbb{R}^n$ is the state vector, $u, y \in \mathbb{R}$ is the system input and output, respectively, $f : \mathbb{R}^n \times \mathbb{R} \to \mathbb{R}^n$ is continuously differentiable in x and continuous in u, $h : \mathbb{R}^n \to \mathbb{R}$.

FRF for *nonlinear* system

Let the $J(x,u) := \frac{\partial f(x,u)}{\partial x}$ be the Jacobian of the system. Assume that there exist symmetric matrices $P > 0$ and $Q > 0$ such that

$$J(x,u)^T P + PJ(x,u) \leq -Q, \ \forall x \in \mathbb{R}^n, u \in \mathbb{R} \tag{6}$$

Then,

- for any bounded input $u(t)$, there is a unique steady-state solution $\bar{x}(t)$, which is bounded.
- if $u(t)$ is produced by the harmonic internal model, then $\bar{x}(t) = \alpha(v,w)$ is also periodic with the same period of the harmonic input but not necessarily sinusoidal

A nonlinear system satisfying the condition (6) is called *convergent* system. The function $\alpha(v,w)$ is termed *Frequency Response Function*.

FRF for *nonlinear* system

Similar to the LTI-system case, consider the internal model for the harmonic input:

$$\begin{aligned} \dot{v} &= S(\omega)v \\ u &= \Gamma v \end{aligned}$$

where

$$v = \begin{bmatrix} v_1 \\ v_2 \end{bmatrix},\ S(\omega) = \begin{bmatrix} 0 & w \\ -w & 0 \end{bmatrix},\ \Gamma = [1\ 0]$$

which in cascade with the nonlinear convergent system

$$\dot{x} = f(x, u)$$

produces the steady-state solution $\bar{x} := \alpha(v, \omega)$.

FRF for *nonlinear* system

The FRF $\alpha(v, \omega)$ cab be obtained by solving the following *nonlinear partial equation*

$$\frac{\partial \alpha(v, \omega)}{\partial v} S(\omega) v = f(\alpha(v, \omega), v_1) \tag{7}$$

In general, this function will depend on both the frequency ω and the amplitude *a*, which is a fundamental property of nonlinear systems.

FRF for *nonlinear* system: Summary [Pavlov *et al.* (2007).]

If the system (5) is convergent, then there exists a uniformly bounded steady-state (UBSS) solution for a certain class of harmonic inputs $u(t) = a\sin(\omega t) \in \Omega_u$, and there exists a nonlinear function $\alpha : \mathbb{R}^3 \to \mathbb{R}^n$ such that

$$\bar{x}(t) := \alpha(v_1, v_2, \omega) \tag{8}$$

which satisfies the following *nonlinear partial equation*

$$\frac{\partial \alpha(v,\omega)}{\partial v} S(\omega) v = f(\alpha(v,\omega), v_1) \tag{9}$$

Bode plot for convergent systems

Now the output response of the system for various amplitude (a) and frequency (ω) inputs can be represented using an amplification gain $\gamma_{a,\omega}$, which is the ratio between the maximal absolute value of the output y at steady-state and the corresponding input signal amplitude, so that

$$\gamma_{a,\omega} = \frac{1}{a}\left(\sup_{v_1^2+v_2^2=a^2} |h\left(\alpha\left(v_1, v_2, \omega\right)\right)|\right) = \frac{1}{a}\left|\overline{y}(t)\right| \tag{10}$$

FRF based identification: Problem formulation

Problem formulation

Design an identifier of the system based on the FRF such that for a given harmonic input it can approximate the amplification gain on a compact set.

Consider

$$\frac{1}{a}\left|\overline{y}_{a,\omega}\right| = \widehat{\gamma}_{a,\omega}\left(\theta\right) + e \tag{11}$$

where $\widehat{\gamma}_{a,\omega}$ is the approximation of $\gamma_{a,\omega}$, θ is the estimator tuning parameters, and $e = \gamma - \widehat{\gamma}$ is the estimation error.

The design goal is to tune θ such that the error e is minimized, hence to achieve a good estimation.

Nonlinear function estimation

Now the identification problem can be explicitly written in terms of FRF estimation by taking $\mathbf{x} = \begin{bmatrix} a & \omega \end{bmatrix}^T \in \mathbb{R}^2$ and $\mathbf{y} = \left|\bar{y}_{a,\omega}\right| \in \mathbb{R}$.

Consider the following regression problem

$$\mathbf{y} = F(\mathbf{x}) \tag{12}$$

where $\mathbf{x} \in \mathbb{R}^{n_i}$ is the input vector, $\mathbf{y} \in \mathbb{R}$ is the observed output, and $F : \mathbb{R}^{n_i} \to \mathbb{R}$ is an unknown smooth nonlinear function. Given a set of N observation sample data, $\Omega_T = \{\mathbf{x}_i, y_i\}_{i=1}^N$, we are interested in estimating $F(\mathbf{x})$, denoted as $\widehat{F}(\mathbf{x})$, by observing the data set Ω_T.

We will discuss here the RBF-NN and the SVM for the nonlinear function estimation.

Radial Basis Function Neural Network (RBF-NN) Approximation

RBF-NN Approximation

Consider an MIMO RBF architecture with n_n hidden neurons. For an input pattern $\mathbf{x}_i$, the corresponding network output is

$$\widehat{F}_{\mathrm{NN}}(\mathbf{x}_i) = \sum_{j=1}^{n_n} w_j \phi_j(\mathbf{x}_i) = \mathbf{w}^{\mathrm{T}} \boldsymbol{\phi}(\mathbf{x}_i) \tag{13}$$

where $\mathbf{x}_i \in \mathbb{R}^{n_i}$ is the input vector, $\widehat{F}_{\mathrm{NN}}$ is the network output, $\mathbf{w} = [w_1, \ldots, w_{n_n}]^{\mathrm{T}} \in \mathbb{R}^{n_n}$ is the output weight vector, $\boldsymbol{\phi}(\mathbf{x}_i) = [\phi_1(\mathbf{x}_i), \ldots, \phi_{n_n}(\mathbf{x}_i)]^{\mathrm{T}} \in \mathbb{R}^{n_n}$ is the vector of basis function with ϕ_j as the response of the j-th neuron to an input.

We use the Gaussian function:

$$\phi_j(\mathbf{x}_i) = \exp\left(-\frac{\left\|\mathbf{x}_i - \boldsymbol{\mu}_j\right\|}{\sigma_j^2}\right) \tag{14}$$

where $\boldsymbol{\mu}_j \in \mathbb{R}^{n_i}$ and σ_j are the center and width of the j-th neuron, respectively and $\|.\|$ denotes the Euclidean norm.

RBF-NN Approximation

Once the number of neurons are determined, the network parameters $(\mathbf{w}, \boldsymbol{\mu}, \sigma)$ might be trained properly. The cost function based on the estimation error for N training samples is defined as

$$\varepsilon = \frac{1}{N} \sum_{i=1}^{N} \left[y_i - \widehat{F}_{\mathrm{NN}}(\mathbf{x}_i) \right]^2 \tag{15}$$

Gradient descent method updates the network parameters in an iterative manner to minimize the cost function. The iteration can be performed by calculating the gradient of the cost function (15) with respect to the network tuning parameters.

RBF-NN Approximation

The weight parameter update at k-th iteration is given as

$$\mathbf{w}[k+1] = \mathbf{w}[k] - \eta_w \frac{\partial \varepsilon_w}{\partial \mathbf{w}} \tag{16}$$

where η_w is the learning rate and the gradient term can be represented in terms of the output error as

$$\frac{\partial \varepsilon_w}{\partial \mathbf{w}} = -\frac{2}{N} \sum_{i=1}^{N} \sum_{j=1}^{n_n} \left(y_i - w_j \phi_j\left(\mathbf{x}_i\right)\right) \phi\left(\mathbf{x}_i\right) \tag{17}$$

RBF-NN Approximation

Similarly the center of the j-th neuron can be tuned as

$$\mu_j[k+1] = \mu_j[k] - \eta_\mu \frac{\partial \varepsilon_{\mu_j}}{\partial \boldsymbol{\mu}_j} \tag{18}$$

where η_μ is the learning rate and the gradient term can be represented in terms of the hidden layer output error as

$$\frac{\partial \varepsilon_{\mu_j}}{\partial \boldsymbol{\mu}_j} = -\frac{2}{N} \sum_{i=1}^{N} \phi_j(\mathbf{x}_i) \frac{(\mathbf{x}_i - \boldsymbol{\mu}_j)}{\sigma_j^2} (y_i - w_j \phi_j(\mathbf{x}_i)) w_j \tag{19}$$

Support Vector Machine (SVM) based Approximation

SVM based Approximation

Consider the SVM for estimating the unknown desired function (5)

$$\widehat{F}_{\mathrm{SV}}(\mathbf{x}_i) = \mathbf{w}^{\mathrm{T}}\varphi(\mathbf{x}_i) + b \tag{20}$$

where $\widehat{F}_{\mathrm{SV}}(\mathbf{x}_i)$ is the SVM output, $\mathbf{w} \in \mathbb{R}^{n_i}$ is the unknown weight vector, $\varphi(\mathbf{x}_i)$ is some nonlinear mapping function of input data, and b is an unknown bias term. The corresponding empirical risk function is

$$\varepsilon_{\mathrm{emp}} = \frac{1}{N}\sum_{i=1}^{N}\left[y_i - \widehat{F}_{\mathrm{SV}}(\mathbf{x}_i)\right] \tag{21}$$

SVM based Approximation

Different cost functions result in different SVM formulations. Vapnik (1995) proposed ϵ-insensitive function which controls the width of the ϵ-insensitive zone, used to fit the training data. Here the problem is to find **w** and b such that the estimation error is bounded by a positive constant ϵ termed as Vapink's insensitive loss function, that is

$$\left|y_i - \widehat{F}_{\mathrm{SV}}(\mathbf{x}_i)\right|_{\epsilon} = \max\left\{0, \left|y_i - \widehat{F}_{\mathrm{SV}}(\mathbf{x}_i)\right| - \epsilon\right\} \tag{22}$$

SVM based Approximation

The straight forward approach to minimize the loss function (22) consists of minimizing the weight vector, resulting in an optimization problem. The corresponding primal problem is

$$\begin{aligned} \min_{\mathbf{w}} \quad & \frac{1}{2}\mathbf{w}^{\mathrm{T}}\mathbf{w} \\ \text{s.t.} \quad & \left| y_i - \left(\mathbf{w}^{\mathrm{T}}\varphi(\mathbf{x}_i) + b\right)\right| \leq \epsilon \end{aligned} \tag{23}$$

SVM based Approximation

Additional slack variables ξ_i and $\widetilde{\xi}_i$ can be used to introduce different constraints for relaxing the restrictions brought by ϵ, thus

$$\min_{\mathbf{w},\xi,\widetilde{\xi}} \quad \frac{1}{2}\mathbf{w}^{\mathrm{T}}\mathbf{w} + \zeta \sum_{i=1}^{N} \left(\xi_i + \widetilde{\xi}_i\right) * \tag{24}$$

$$\text{s.t.} \quad -\left(\epsilon + \xi_i^*\right) \leq y_i - \left(\mathbf{w}^{\mathrm{T}}\varphi(\mathbf{x}_i) + b\right) \leq \epsilon + \xi_i \tag{25}$$

where $\zeta > 0$ is the regularization parameter.

SVM based Approximation

Generally, it may be difficult to solve the primal problem directly. The dual formulation can be utilized to facilitate the resolvability. The standard Lagrangian function is used to derive the dual problem. In that case, one can solve the dual problem first and then derive solution for the primal problem. The Lagrange function of the primal problem (24) is

$$\begin{aligned}
\mathcal{L} \;=\; & \frac{1}{2}\mathbf{w}^{\mathrm{T}}\mathbf{w} + \zeta \sum_{i=1}^{N} \left(\xi_i + \widetilde{\xi}_i\right) - \sum_{i=1}^{N} \left(\eta_i \xi_i + \widetilde{\eta}_i \widetilde{\xi}_i\right) \\
& - \sum_{i=1}^{N} \alpha_i \left[\left(\mathbf{w}^{\mathrm{T}}\varphi(\mathbf{x}_i) + b\right) - y_i + \epsilon + \xi_i\right] \\
& - \sum_{i=1}^{N} \widetilde{\alpha}_i \left[y_i - \left(\mathbf{w}^{\mathrm{T}}\varphi(\mathbf{x}_i) + b\right) + \epsilon + \widetilde{\xi}_i\right] \qquad (26)
\end{aligned}$$

where $\alpha, \widetilde{\alpha}, \eta, \widetilde{\eta} \geq 0$ are the Lagrange multipliers.

SVM based Approximation

The minimization of the (24) is equivalent to the maximization of minimum of its Lagrange function (26). Finding optimal condition w.r.t the primal variables $\mathbf{w}, b, \xi, \widetilde{\xi}$ yields

$$\frac{\partial \mathcal{L}}{\partial \mathbf{w}} = 0 \implies \sum_{i=1}^{N} (\alpha_i - \widetilde{\alpha}_i)\, \varphi(\mathbf{x}_i) = \mathbf{w} *$$

$$\frac{\partial \mathcal{L}}{\partial b} = 0 \implies \sum_{i=1}^{N} (\alpha_i - \widetilde{\alpha}_i) = 0$$

$$\frac{\partial \mathcal{L}}{\partial \boldsymbol{\xi}} = 0 \implies \zeta - \alpha_i - \eta_i = 0$$

$$\frac{\partial \mathcal{L}}{\partial \widetilde{\boldsymbol{\xi}}} = 0 \implies \zeta - \widetilde{\alpha}_i - \widetilde{\eta}_i = 0$$

SVM based Approximation

The primal variables can be now eliminated by plugging (27) in (26) and further simplification yields the following dual problem

$$\max_{\alpha,\widetilde{\alpha}} \begin{cases} -\frac{1}{2}\sum_{i,j=1}^{N}\left(\alpha_i-\widetilde{\alpha}_i\right)\left(\alpha_j-\widetilde{\alpha}_j\right)K(\mathbf{x}_i,\mathbf{x}_j) \\ -\epsilon\sum_{i=1}^{N}\left(\alpha_i+\widetilde{\alpha}_i\right)+\sum_{i=1}^{N}y_i\left(\alpha_i-\widetilde{\alpha}_i\right) \end{cases}$$

$$\text{s.t.} \quad \sum_{i=1}^{N}\left(\alpha_i-\widetilde{\alpha}_i\right)=0 \text{ and } \alpha_i,\widetilde{\alpha}_i\in[0,\zeta]$$

which is a constrained convex quadratic optimization problem.

SVM based Approximation

Here $K(\mathbf{x}_i, \mathbf{x}_j) = \varphi(\mathbf{x})^{\mathrm{T}} \varphi(\mathbf{x})$ is termed as the Kernel function, used to model the inputs into higher dimensional feature space, which allows to obtain features with higher-order correlations between input variables.

There exist many Kernel functions, which satisfy the Mercer's condition (Smola (2004)). Here we consider the RBF given in (14) as the Kernel function, which guarantees an adequate accuracy in the nonlinear function estimation problems.

SVM based Approximation

Finally, the estimation function (20) can be rewritten as follows

$$\widehat{F}_{\mathrm{SV}}(\mathbf{x}_t) = \sum_{i=1}^{N} (\alpha_i^* - \widetilde{\alpha}_i^*)\, K(\mathbf{x}_i, \mathbf{x}_t) + b^* \tag{27}$$

where $()^*$ indicates optimal values obtained by solving (27), $\mathbf{x}_t$ is the new test data, and

$$b^* = \frac{1}{N_z} \sum_{j=1}^{N_z} \sum_{i=1}^{N} \left[y_j - (\alpha_i^* - \widetilde{\alpha}_i^*)^{\mathrm{T}} K(\mathbf{x}_i, \mathbf{x}_j) - \epsilon \right] \tag{28}$$

for j with $0 < \alpha_j^*, \widetilde{\alpha}_j^* < \zeta$.

SVM based Approximation

In contrast with the choice of the number of neurons in RBF-NN case, the number of support vectors is directly derived by solving the optimization problem. The support vectors are the data points that lie outside the ϵ-insensitive zone, thus for the points where $\left| y_i - \widehat{F}_{\mathrm{SV}}(\mathbf{x}_i) \right| - \epsilon > 0$. Hence, the number of support vectors changes for different choice of ϵ. Decreasing ϵ increases the number of support vectors, and vice versa. In some cases such as v-SVM (Smola (2004)), the user can specify the number of support vectors.

Simulation example

Simulations on a 1 DOF mechanical system

Consider a one degree-of-freedom mechanical system with a nonlinear cubic damping term (c_{nl})

$$\begin{aligned} m\ddot{q} + c\dot{q} + c_{nl}\dot{q}^3 + kq &= d \\ y &= q \end{aligned} \tag{29}$$

It can be shown that this system is convergent. In the simulations, the system parameters were set as: $m = 1\mathrm{kg}$, $c = 0.4\mathrm{Ns/m}$, $k = 36\mathrm{N/m}$ and $c_{nl} = 0.8\mathrm{Ns}^3/\mathrm{m}^3$.

Simulations on a 1 DOF mechanical system

The following figure shows the forced response of the system (45), where the solutions for different initial conditions

$$q_1(0) = 0.3, q_2(0) = 0.1, q_3(0) = -0.3$$

converge to the unique steady-state solution exponentially. Due to this convergence property, the FRF from the steady-state response can be derived without concerning the initial conditions.

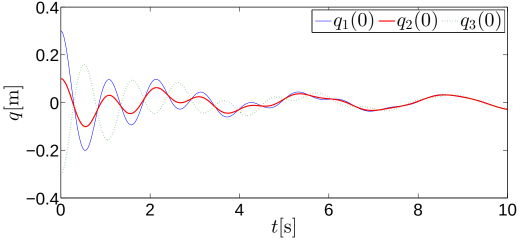

Figure: Convergence of trajectories for different initial conditions.

Simulations on a 1 DOF mechanical system

The amplitude and frequency range of the input excitation:

$$a \in [0.5, 6]\,\mathrm{N}, \quad \omega \in [3, 9]\,\mathrm{rad/s}.$$

Using these inputs (a combination of 25 amplitude points and 31 frequency points), 775 data points were generated via numerical simulation, and the Bode plot is shown in the following

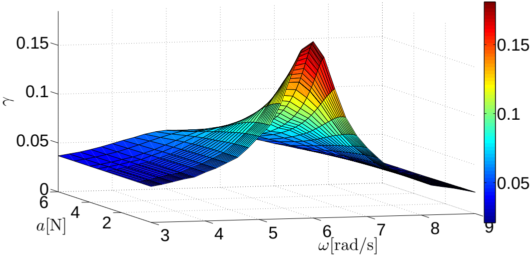

Figure: Actual FRF of the system.

Training RBF-NN

We constructed three different estimation models:

- RBF_1 model was trained using $\Omega_{\mathrm{T}96}$, where only the output weights are tuned.
- RBF_2 model was trained using $\Omega_{\mathrm{T}208}$, where only the output weights are tuned.
- RBF_3 model was trained using $\Omega_{\mathrm{T}208}$, where both the weights and centers are tuned.

Training SVM

For SVM, two estimation models were constructed:

- SVM_1 trained using Ω_{T96}
- SVM_2 trained using Ω_{T208}

Simulation results for RBF_1

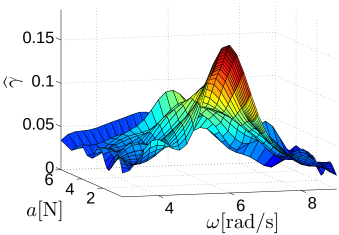

(a) Estimated FRF

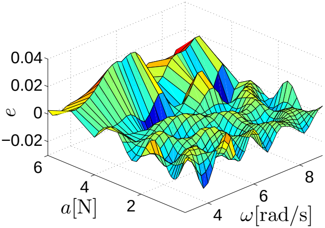

(b) Error

Figure: Simulation results for RBF_1.

Simulation results for RBF_2

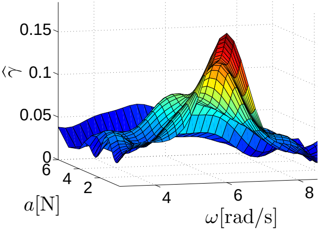

(a) Estimated FRF

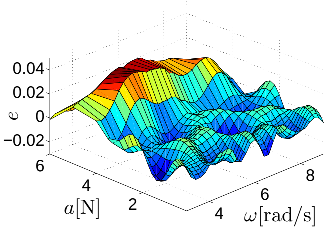

(b) Error

Figure: Simulation results for RBF_2.

Simulation results for RBF_3

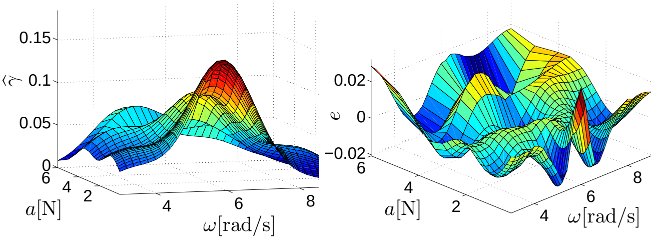

(a) Estimated FRF (b) Error

Figure: Simulation results for RBF_3.

Simulation results for SVM_1

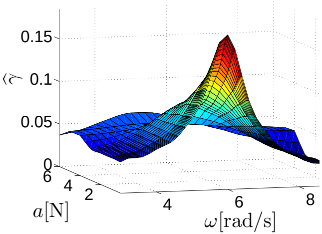

(a) Estimated FRF

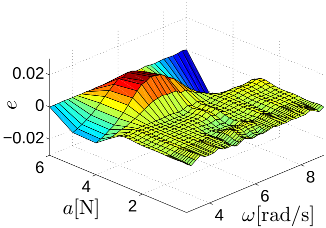

(b) Error

Figure: Simulation results for SVM_1.

Simulation results for SVM_2

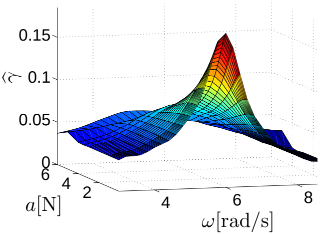

(a) Estimated FRF

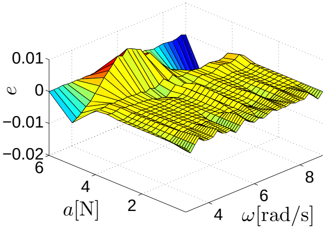

(b) Error

Figure: Simulation results for SVM_2.

Training results

- RBF-NN's are sensitive to the initial values of the network parameter.
- SVM's have less parameters need to be initialized.
- SVM's does not give rise to local minima.
- A better accuracy is achieved with the SVM.
- The number of iterations in SVM is much less in RBF-NN.

Model	**Training Speed**		**MSE**	
	Iteration	CPU Time	Training	Testing
RBF_1	$3,500$	5.16 min	2.03×10^{-5}	9.42×10^{-5}
RBF_2	$6,500$	12.7 min	2.61×10^{-5}	4.62×10^{-5}
RBF_3	$11,000$	19.6 min	6.04×10^{-5}	6.67×10^{-5}
SVM_1	16	0.29 sec	1.00×10^{-10}	2.58×10^{-6}
SVM_2	21	1.83 sec	1.02×10^{-10}	3.24×10^{-7}

FRF based adaptive control

Problem

Consider the following nonlinear time-invariant mechanical system

$$\dot{x} = f(x, \tau) + \Gamma u + \Lambda w \quad (31)$$

$$y = g(x) \quad (32)$$

where τ is the control input, u vibration control input and w unknown harmonic disturbance.

Depending on whether the system is convergent, following two cases are present:

1. The open-loop system $f(x, 0)$ is already convergent: no control action τ is needed.
2. The open-loop system $f(x, 0)$ is not convergent: a controller τ needs to be designed such that the inner closed-loop system $f(x, \tau)$ becomes convergent.

Vibration control through FRF compensation

Let us consider a controller of form

$$u = -\Theta x \tag{33}$$

where $\Theta \in \mathbb{R}^{n_q \times n}$ is a state feedback controller gain matrix.

The control objective is to find a frequency response based updating law Ψ for the controller gain

$$\dot{\Theta} = \Psi(F) \tag{34}$$

where F is FRF of the system obtained for the band of interest, such that a desired vibration attenuation is achieved for the closed-loop system (31) without loosing the convergence property of the overall system.

Mechanical systems

Consider a mechanical system with an active controller u

$$M\ddot{q} + C\dot{q} + Kq + \Phi(\dot{q}) = \Gamma u + \Lambda w \tag{35}$$

where $M,\ C,\ K$ are symmetric positive-definite matrices corresponding to the mass, damping, and stiffness respectively, $\ddot{q},\ \dot{q}$ and $q \in \mathbb{R}^{n_q}$ are the acceleration, velocity, and position vectors, respectively, and $\Phi(\dot{q}) : \mathbb{R}^{n_q} \to \mathbb{R}^{n_q}$ satisfies the following assumption

$$\Phi_J(\dot{q}) := \frac{\partial \Phi(\dot{q})}{\partial \dot{q}} \geq 0,\ \Phi(0) = 0 \tag{36}$$

The class of mechanical system (35) with a smooth nonlinearity that satisfies (36) is convergent.

PD controller

Consider the PD controller

$$u = -\Theta_p e - \Theta_d \dot{e} \tag{37}$$

where $\Theta_p, \Theta_d \in \mathbb{R}^{n_q \times n_q}$ are diagonal matrices corresponding to the proportional and derivative gains, respectively, $e = q - q^d$ corresponds to the position error, $\dot{e} = \dot{q} - \dot{q}^d$ corresponds to the velocity error, and q^d is the desired position. In active vibration control case (regulation), the references are $q^d = \dot{q}^d = 0$, hence (37) becomes

$$u = -\Theta_p q - \Theta_d \dot{q} \tag{38}$$

PD controller

The closed-loop system (35) with the PD controller (38) is

$$M\ddot{q} + C\dot{q} + Kq + \Phi(\dot{q}) = \Lambda w - \Theta_p q - \Theta_d \dot{q} \tag{39}$$

which can be written in the state-space form as

$$\begin{bmatrix} \dot{x}_1 \\ \dot{x}_2 \end{bmatrix} = \begin{bmatrix} x_2 \\ -M^{-1}\left[\ (C + \Theta_d)\, x_2 + (K + \Theta_p)\, x_1 + \Phi(x_2) - \Lambda w\ \right] \end{bmatrix} \tag{40}$$

PD controller

The range of gains for which the system is convergent is defined in the following theorem.

Theorem

Consider the class of nonlinear system (35) with a bounded external excitation w controlled using the control law (33). If we choose the control gains such that $\Theta = [\Theta_p \ \Theta_d] \in \Omega_\Theta \subset \mathbb{R}_+^\Theta$, then the closed-loop system (39) is convergent in Ω_x and the state trajectories exponentially converge to a unique steady-state solution from any initial conditions.

FRF based adaptive controller

The amplification gain $\gamma_{a,\omega}$ of the system, for a range of amplitudes ($a \in [\underline{a}, \overline{a}] \in \mathbb{R}^{n_a}$) and frequencies ($\omega \in [\underline{\omega}, \overline{\omega}] \in \mathbb{R}^{n_\omega}$) can be represented in a matrix form as

$$\mathcal{F}_0 = \begin{bmatrix} \gamma_{\underline{a},\underline{\omega}} & \cdots & \gamma_{\underline{a},\overline{\omega}} \\ \vdots & \ddots & \vdots \\ \gamma_{\overline{a},\underline{\omega}} & \cdots & \gamma_{\overline{a},\overline{\omega}} \end{bmatrix} \in \mathbb{R}^{n_a \times n_\omega} \tag{41}$$

The above matrix can be considered as the open-loop FRF matrix of the system. Now $\mathcal{F}_0$ can be analyzed in order to get a knowledge about the critical amplitudes and frequencies of the excitation input, at which the system possess a larger amplification gain.

FRF based adaptive controller

One way to evaluate the FRF matrix is by finding its Frobeinus norm (F-norm), which are sensitive towards its each elements. F-norm of the FRF matrix F can be calculated as

$$\|\mathcal{F}\|_{\mathrm{F}} = \sqrt{\sum_{r=1}^{n_a} \sum_{s=1}^{n_\omega} |\gamma_{r,s}|^2} = \sqrt{\mathrm{tr}\left(\mathcal{F}^{\mathrm{T}}\mathcal{F}\right)} \geq 0 \tag{42}$$

FRF based adaptive controller

The steady-state output of the closed-loop system for a particular value of proportional and derivative gains can be represented as $\bar{y}_w(t, \Theta)$. The amplification gain of the closed-loop system, denoted by $\gamma_{a,\omega}(\Theta)$, satisfies the following relation

$$|\bar{y}_w(t, \Theta)| = \gamma_{a,\omega}(\Theta)\,|a| \tag{43}$$

Hence the peak vibration output of the system can be attenuated by minimizing the amplification gains. Using the amplification gains obtained under a range of excitation, the closed-loop FRF matrix, $\mathcal{F}_\Theta$ can be constructed as given in (41). The control objective is to minimize the FRF magnitude such that

$$\|\mathcal{F}_\Theta\|_{\mathrm{F}} = \sqrt{\sum_{r=1}^{n_a}\sum_{s=1}^{n_\omega} |\gamma_{r,s}(\Theta)|^2} \le \vartheta < \|\mathcal{F}_0\|_{\mathrm{F}}$$

where ϑ is a measure of acceptable vibration range.

FRF based adaptive controller

The new controller gains are

$$\Theta_{i+1} = \Theta_i + \gamma \mathbf{F}_i \epsilon_i \tag{44}$$

The above adaptation scheme is used to calculate the new controller gains (Θ_{i+1}), based on the closed-loop system's FRF $\left(\mathcal{F}_{\Theta,i}\right)$ obtained using the previous controller gains (Θ_i). When the error ϵ_i is positive, the gains will increase and for negative *epsilon* the gain decreases. Based on the γ, the gains will adapt over each iteration until a satisfactory vibration attenuation is achieved for a band of excitation, that is $\|\mathcal{F}_\Theta\|_{\mathrm{F}} = \theta$, hence $\epsilon_i \to 0$ as $i \to \infty$.

One DOF mechanical system with a cubic nonlinearity

Consider a one DOF mechanical system with a cubic nonlinearity

$$m\ddot{q} + c\dot{q} + \xi\dot{q}^3 + kq = w \tag{45}$$

where $q, \dot{q}$, and $\ddot{q}$ the relative displacement, velocity, and acceleration of the mass. The system parameters are set as:
$m = 1\text{kg}, c = 0.4\text{Ns}/\text{m}, \xi = 0.7\text{Ns}^3/\text{m}^3$, and $k = 36\text{N}/\text{m}$. All the control actions were employed at a sampling period of 10ms.

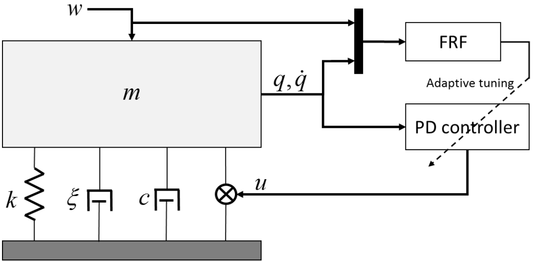

Figure: Block diagram of the proposed active vibration control system.

One DOF mechanical system with a cubic nonlinearity

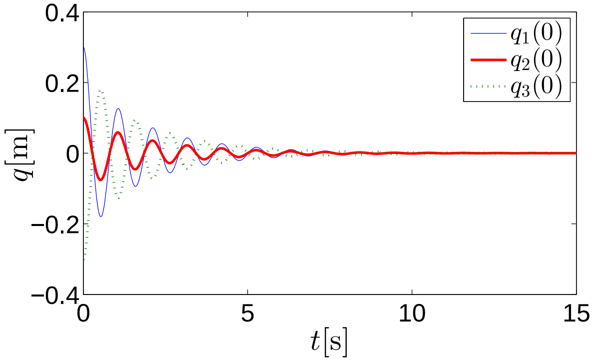

Figure: Convergence of trajectories for different initial conditions ($q_1(0) = 0.3, q_2(0) = 0.1, q_3(0) = -0.3$): (a) natural response

One DOF mechanical system with a cubic nonlinearity

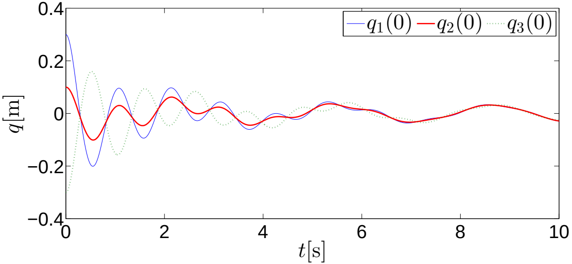

Figure: Convergence of trajectories for different initial conditions ($q_1(0) = 0.3, q_2(0) = 0.1, q_3(0) = -0.3$): (b) forced response ($a = 1\text{N}$ and $\omega = 2$ rad/s).

One DOF mechanical system with a cubic nonlinearity

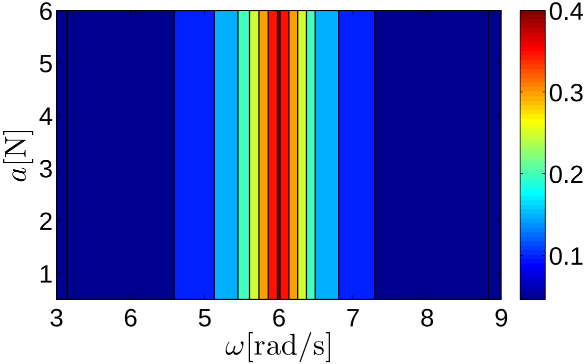

Figure: Contour plot of the open-loop FRF ($\mathcal{F}_0$) of the mechanical system: (a) linear case ($\xi = 0$)

One DOF mechanical system with a cubic nonlinearity

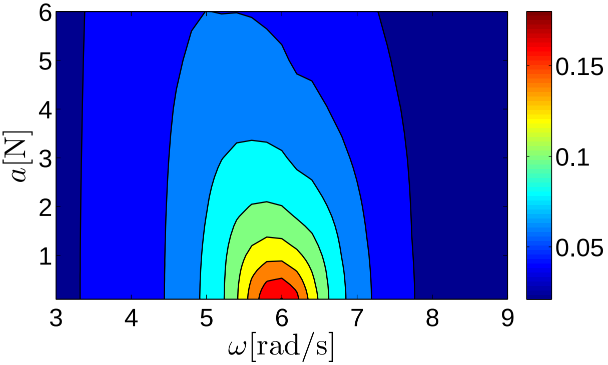

Figure: Contour plot of the open-loop FRF ($\mathcal{F}_0$) of the mechanical system: (b) nonlinear case ($\xi = 0.7$).

The active control scheme can adapt to these nonlinear effects. The closed-loop system is

$$m\ddot{q} + c\dot{q} + \xi\dot{q}^3 + kq = w - \theta_p q - \theta_d \dot{q} \tag{46}$$

The effects of adaptive PD controller on the performance of the active vibration control system are investigated. The adaptive algorithm parameters are set as: $\Upsilon = [200\ 5]$, $\Theta_\mathrm{p} = 0.5$, $\Theta_\mathrm{d} = 3$, and $\Theta_{\min} = [0.001\ 0.001]$. The controller gains was started from a minimal value $\Theta_{t_0} = \Theta_{\min}$, and allowed to adapt using the update law after each set of FRF is calculated.

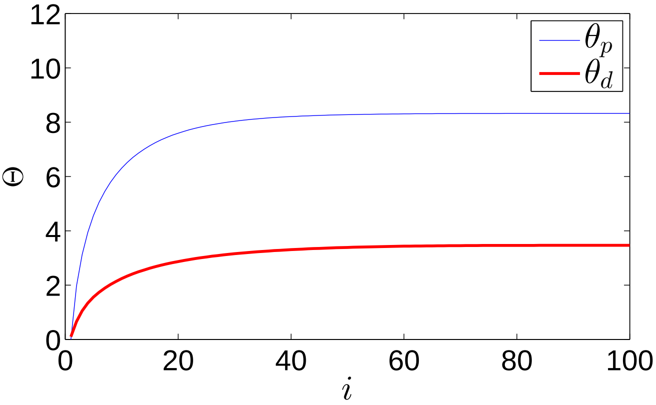

Figure: Evolution of the adaptation parameters over each iteration: (a) gain.

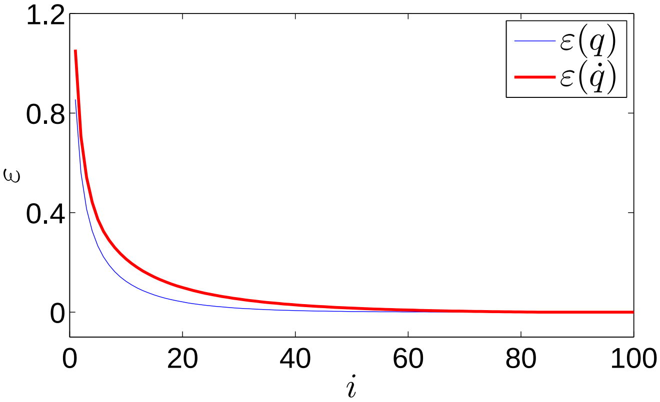

Figure: Evolution of the adaptation parameters over each iteration: (b) error.

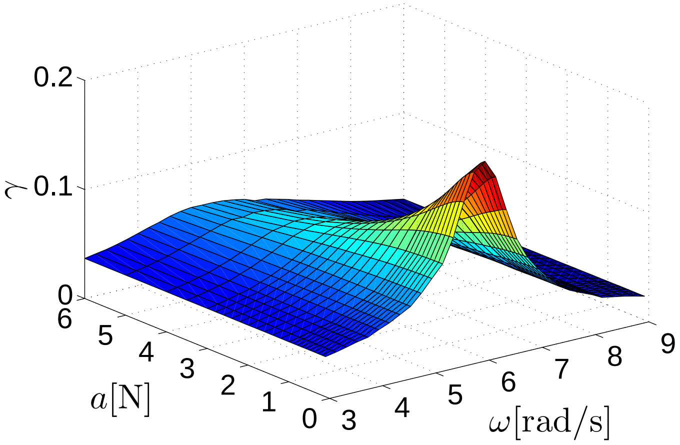

Figure: Comparison between the FRF: (a) open-loop case

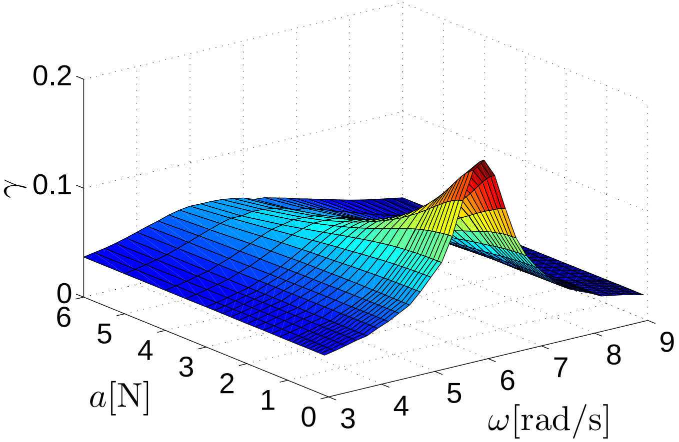

Figure: Comparison between the FRF: (b) closed-loop case.

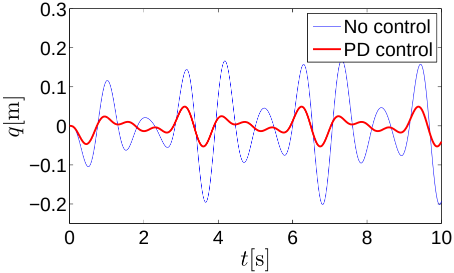

Figure: Time response comparison between the uncontrolled and controlled displacements of the closed-loop system.

Application to Satellite Attitude Control Problem

Application to Satellite Attitude Control Problem

Application to Satellite Attitude Control Problem

Momentum type actuators such as Reaction Wheels (RW) are widely used as attitude control actuators in spacecraft for orbital maneuvering. Unfortunately, these actuators are one of the main source of on-board vibration (Masterson (2002)), which is caused by the static and dynamic imbalances in the RW assembly. This can be critical for the high precision space applications such as high-sensitivity imaging and astrometry.

Attitude model

The dynamics and kinematics of a satellite system can be modelled as

$$\mathbf{H}\dot{\boldsymbol{\omega}}_{\boldsymbol{s}} + \mathbf{S}(\boldsymbol{\omega}_{\boldsymbol{s}})\mathbf{H}\boldsymbol{\omega}_{\boldsymbol{s}} = \tau \tag{47}$$

$$\dot{\mathbf{q}} = \mathbf{J_s}\omega_{\mathbf{s}} \tag{48}$$

where $\mathbf{H} \in \mathbb{R}^{3\times 3}$ is the inertia matrix, $\boldsymbol{\omega}_{\boldsymbol{s}} \in \mathbb{R}^3$ is the angular velocity vector, $\mathbf{S}(\boldsymbol{\omega}_{\boldsymbol{s}})\mathbf{H}$ is the angular momentum with the skew-symmetric matrix $\mathbf{S}(.)$ representing the vector cross product, $\tau \in \mathbb{R}^3$ is the torque applied to the satellite system, $\mathbf{q} \in \mathbb{R}^3$ is the satellite attitude vector, and $\mathbf{J_s}(\omega_{\mathbf{s}}) \in \mathbb{R}^{3\times 3}$ is the Jacobian matrix, all expressed in the satellite body frame. The Modified Rodrigues parameters were used to represent the kinematic equations of the satellite system.

Attitude model

By considering $\mathbf{q}$ and $\dot{\mathbf{q}}$ as the state-space coordinates and using (48), the equation of motion of the satellite system (47) can be written in the Lagrangian form as

$$\mathbf{H_s}(\mathbf{q})\ddot{\mathbf{q}} + \mathbf{C_s}(\mathbf{q}, \dot{\mathbf{q}})\dot{\mathbf{q}} = \mathbf{u_s} \tag{49}$$

where

$$\begin{aligned} \mathbf{H_s}(\mathbf{q}) &= \mathbf{J_s}^{-\mathrm{T}}\mathbf{H}\mathbf{J_s}^{-1} \\ \mathbf{C_s}(\mathbf{q}, \dot{\mathbf{q}}) &= \mathbf{J_s}^{-\mathrm{T}}\mathbf{H}\mathbf{J_s}^{-1}\dot{\mathbf{J}}_\mathbf{s}\mathbf{J_s}^{-1} - \mathbf{J_s}^{-\mathrm{T}}\mathbf{S}(\omega_\mathbf{s})\mathbf{H}\mathbf{J_s}^{-1} \\ u_\mathbf{s} &= \mathbf{J_s}^{-\mathrm{T}}\boldsymbol{\tau} \end{aligned}$$

Since the system (49) verifies the structure and skew-symmetric property (Slotine (1990)), it satisfies the theoretical analysis.

Disturbances

The rotational elements of the RW generates periodic disturbances, which can be modelled as a series of discrete harmonics Masterson (2002)

$$w_{\mathrm{rw}} = \sum_{l=1}^{\bar{h}} \tilde{a}_l \nu^2 \sin\left(2\pi h_l \nu t + \varphi_l\right) \tag{50}$$

where $\bar{h}$ is the total number of harmonics, $\tilde{a}_l$ is the amplitude coefficient of the l-th harmonic, ν is the wheel speed, h_l is the l-th harmonic number and φ_l is a random phase. Now the satellite model with the disturbance w_{rw} can be represented as

$$\mathbf{H}\dot{\boldsymbol{\omega}}_{\mathbf{s}} + \mathbf{S}(\boldsymbol{\omega}_{\mathbf{s}})\mathbf{H}\boldsymbol{\omega}_{\mathbf{s}} = \tau + \mathbf{u} + \Lambda w_{\mathrm{rw}} \tag{51}$$

where $\mathbf{u}$ is generated by the proposed FRF-based adaptive control algorithm for minimizing the vibration signals caused by the RW assembly.

The block diagram of the implementation of the proposed algorithm is shown

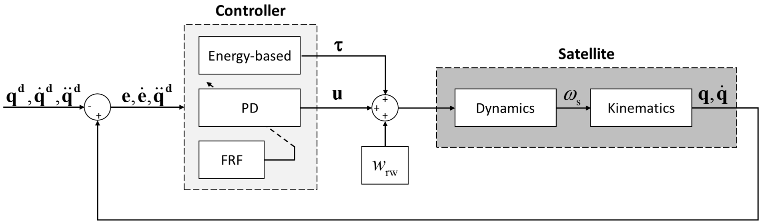

Figure: Block diagram of the active vibration control system for satellites.

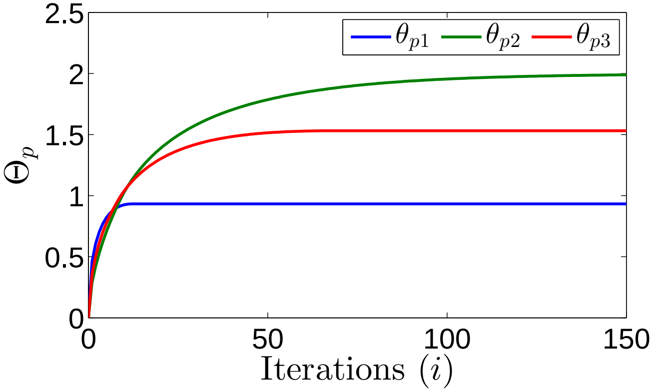

Figure: Evolution of the adaptive gains over each iteration: (a) proportional gain

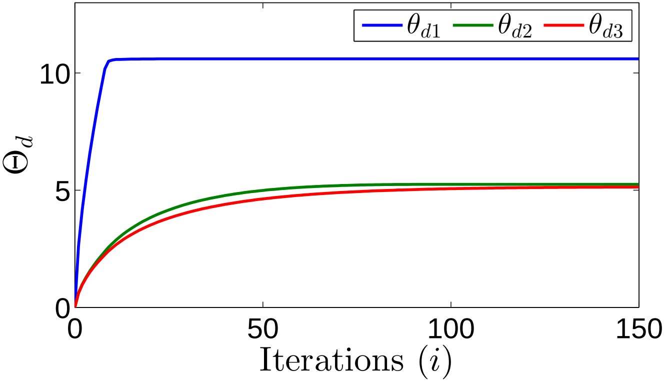

Figure: Evolution of the adaptive gains over each iteration: (b) derivative gain.

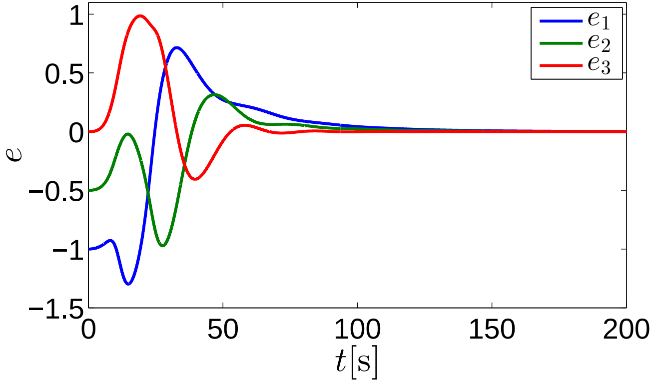

Figure: Error of the satellite attitude in the presence of disturbance without adaptive controller: (a) position error.

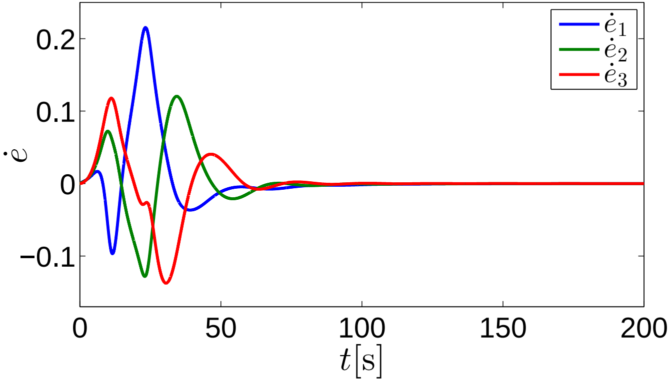

Figure: Error of the satellite attitude in the presence of disturbance without adaptive controller:(b) velocity error.

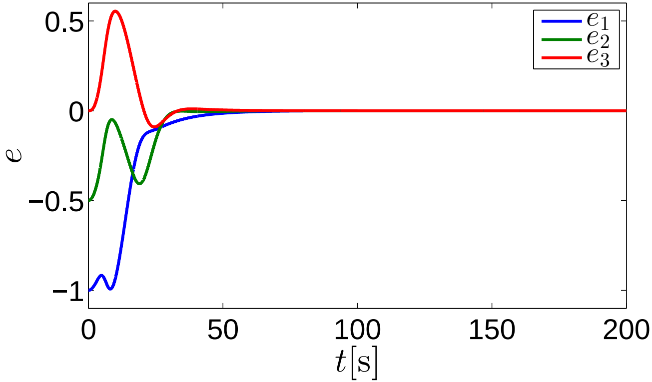

Figure: Error of the satellite attitude in the presence of disturbance with adaptive controller: (a) position error

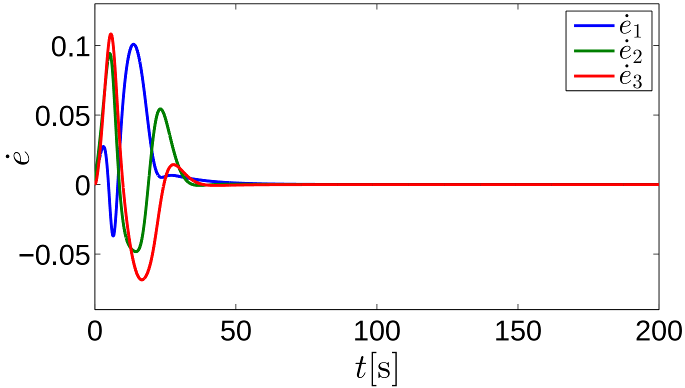

Figure: Error of the satellite attitude in the presence of disturbance with adaptive controller:(b) velocity error.

Conclusions

- The frequency response function (FRF) has been extended to the class of nonlinear convergent systems.
- Identification for this class of nonlinear system is done by estimating the FRF.
- Adaptive vibration control is designed by minimizing the FRF from the disturbances to the output.
- Satellite attitude control is taken as an illustrating example.

THANKS!